iScience

CellPress
OPEN ACCESS

Article

A small molecule that selectively inhibits the growth of Epstein-Barr virus-latently infected cancer cells

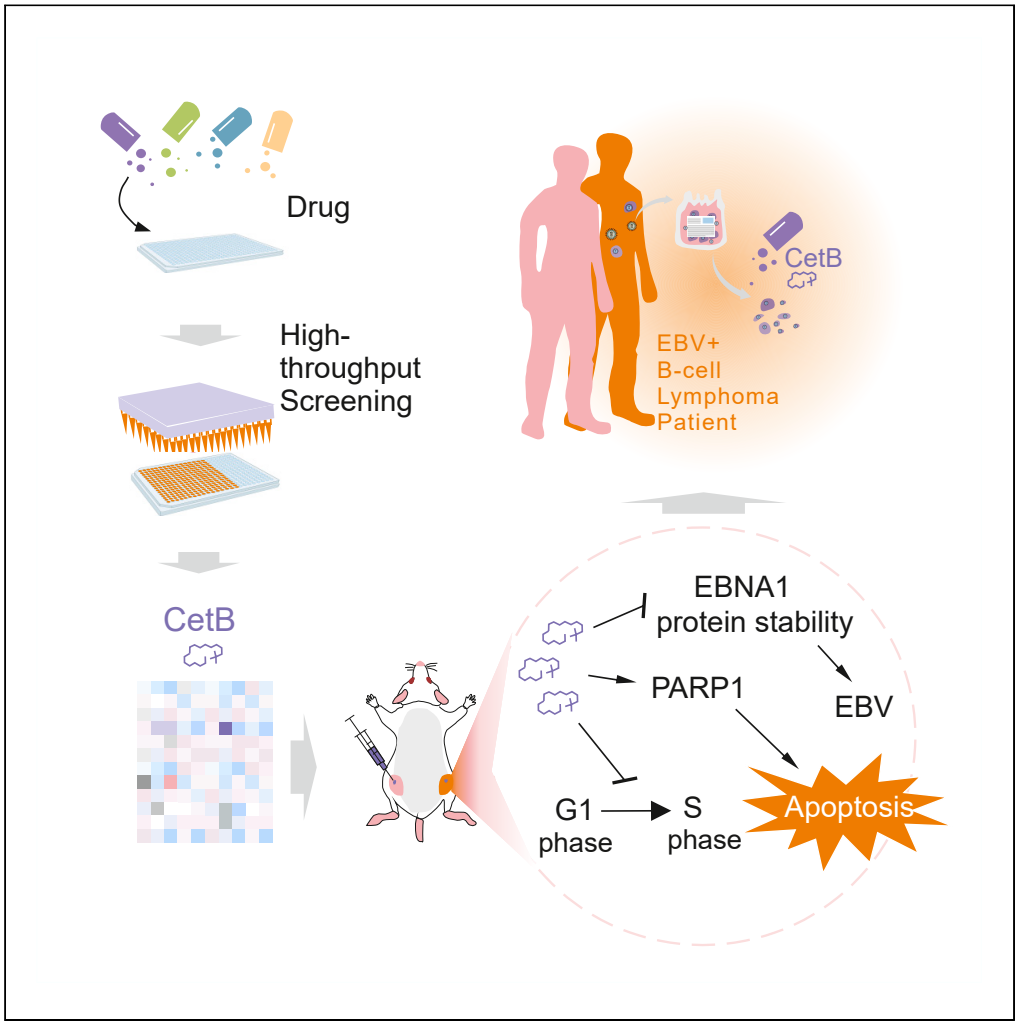

Ying Li, Shujuan Du, Kun Zhou, ..., Fang Wei, Yin Tong, Qiliang Cai

zhangdzyky@163.com (D.Z.)
fangwei@sjtu.edu.cn (F.W.)
tongyin_cn2@hotmail.com (Y.T.)
qiliang@fudan.edu.cn (Q.C.)

Highlights

CetB selectively inhibits EBV-infected B lymphoma and NPC cell growth

CetB reduces EBNA1 protein stability and activates G1 arrest for apoptosis

CetB is a potential compound specific against EBV-associated cancers

Li et al., iScience 27, 110581
September 20, 2024
https://doi.org/10.1016/j.isci.2024.110581

iScience

CellPress
OPEN ACCESS

Article

A small molecule that selectively inhibits the growth of Epstein-Barr virus-latently infected cancer cells

Ying Li,[1,4] Shujuan Du,[2,4] Kun Zhou,[1,4] Yulin Zhang,[1,4] Xiaoting Chen,[2] Caixia Zhu,[2] Yuping Jia,[3] Yuyan Wang,[2] Daizhou Zhang,[3,*] Fang Wei,[1,*] Yin Tong,[1,*] and Qiliang Cai[2,5,*]

SUMMARY

Epstein-Barr virus (EBV), an oncogenic herpesvirus, is predominantly found in the latent infection form and is highly associated with many human malignancies, which mainly have poor prognoses and no effective treatments. Here, we obtained thirteen compounds from small-molecule libraries for specific inhibition of EBV-latently infected cell growth *in vitro* by high-throughput screening. Among them, cetrimonium bromide (CetB) was identified to selectively inhibit the growth of different EBV-infected B lymphoma cell lines. Importantly, CetB reduced EBNA1 protein stability, activated G1 arrest and early apoptosis of EBV-latently infected cells without viral lytic reactivation, which leads to dramatically inhibit colony formation and tumor growth of EBV-infected cells *in vitro* and *in vivo*, and significantly prolong the survival of tumor-bearing mice. Overall, these findings demonstrate that CetB acts as a highly selective inhibitor of the growth of EBV-infected cells and has the potential for further development of effective therapeutic strategies specific against EBV-associated cancers.

INTRODUCTION

Epstein-Barr virus (EBV), an oncogenic gamma-herpesvirus,[1] was first discovered in 1964 by Epstein and Barr in African children with Burkitt's lymphoma.[2] EBV is a ubiquitous human virus that maintains an overall infection rate of around 95% in humans,[3] and can persist in individuals for life after the primary infection, which mostly occurs in childhood and without obvious clinical symptoms.[1] In contrast to other herpes viruses, EBV can cause B cell transformation and is closely related to a variety of malignant tumors, such as Hodgkin's lymphoma (HL), Burkitt's lymphoma (BL), diffuse large B cell lymphoma (DLBCL), and post-transplant lymphoproliferative disease (PTLD).[4,5] Clinically, EBV-related tumors have three typical characteristics, including extensiveness, seriousness, and refractory to treatment. For example, EBV can accelerate tumor progression, with poor patient prognosis.[6] Patients with post-transplant lymphoproliferative diseases with a high EBV copy number exhibit rapid progression, a high degree of malignancy, and a mortality rate of nearly 50%; this is especially true for pediatric transplant recipients, who are vulnerable to EBV due to the immaturity of the pre-transplant immune system and may acquire the virus from donor organs with maximum immunosuppression.[7] In HL, the EBV-DNA load in plasma is highly consistent with tumor burden, and a high EBV-DNA load in plasma is often associated with poor prognosis.[8] In addition, increasing evidence shows that EBV-positive patients with DLBCL also have a worse prognosis than EBV-negative patients.[9]

It has been well demonstrated that the life cycle of EBV contains latent and lytic replication phases. During latency, six nuclear antigens including EBNA1, EBNA2, EBNA3A/3B/3C, and EBNA-LP and three latent membrane proteins (LMP1, LMP2A, and LMP2B) are varied expressed dependent,[10] which are generally considered key for virus-induced tumorigenesis. The high perennial latent EBV carrier rate allows reactivation into lytic replication for virion production by factors including the alternation of the host immune suppression, stress stimulation, or expression of viral proteins and non-coding RNAs.[11] In past decades, the role of EBV infection in the development and progression of many malignancies has been extensively demonstrated. However, there remains a lack of efficient and specific treatment for EBV-related cancers, and no inhibitors effective against EBV latent infection have emerged thus far.[12] Although many antiviral agents, such as acyclovir and ganciclovir, are potent inhibitors of herpesvirus replication, none of them have been approved by the Food and Drug Administration (FDA) or European Medicines Agency for the treatment of EBV infection in clinical practice.[13] In addition, because these antiviral agents mainly target

[1]Division of Hematology, Shanghai First People's Hospital, School of Medicine & ShengYushou Center of Cell Biology and Immunology, Joint International Research Laboratory of Metabolic & Development Sciences, School of Life Sciences and Biotechnology, Shanghai Jiao Tong University, Shanghai 200240, P.R. China
[2]MOE/NHC/CAMS Key Laboratory of Medical Molecular Virology, Shanghai Institute of Infections Disease and Biosecurity, Shanghai Frontiers Science Center of Pathogenic Microorganisms and Infection, School of Basic Medical Sciences, Shanghai Medical College, Fudan University, Shanghai 200032, P.R. China
[3]Shandong Academy of Pharmaceutical Sciences, Jinan 250100, P.R. China
[4]These authors contributed equally
[5]Lead contact
*Correspondence: zhangdzyky@163.com (D.Z.), fangwei@sjtu.edu.cn (F.W.), tongyin_cn2@hotmail.com (Y.T.), qiliang@fudan.edu.cn (Q.C.)
https://doi.org/10.1016/j.isci.2024.110581

DNA polymerase to reduce the replication of the EBV lytic phase, and given that the process of EBV latent infection does not require DNA polymerase, their antiviral effects are suboptimal.[14] Therefore, the development of a novel strategy to discover compounds targeting EBV latent infection is urgently required.[12]

In this study, we performed high-throughput screening of 3,988 standard compounds and natural products to identify inhibitors targeting EBV latently infected cancer cells. We used several pairs of EBV-infected and -uninfected B lymphoma cell lines with the same genotypic background to offer parallel infected and uninfected cells for comparative screening. Finally, we identified cetrimonium bromide (CetB) as a promising candidate for selectively targeting EBV latently infected B lymphoma and nasopharyngeal carcinoma (NPC) cell growth, as well as peripheral primary B cell growth from patients with EBV-positive DLBCL. CetB was also found to effectively inhibit colony formation and tumor growth of EBV-infected B cell lymphoma cells *in vitro* and *in vivo*, and significantly prolonged the survival of tumor-bearing mice. Mechanistically, we found that CetB selectively induced G1 arrest and early apoptosis of EBV-latently infected B lymphoma cells. CetB was shown to reduce EBNA1 protein stability, but not activate ZTA expression for lytic replication. Our findings provide a highly selective inhibitor and the potential for further development of effective therapeutic strategies specific against EBV-associated cancers.

RESULTS

Identification of small-molecule inhibitors of EBV latently infected cancer cells

To identify inhibitors that can efficiently target and selectively kill EBV latently infected cancer cells, we conducted high-throughput screening with libraries of small molecules using EBV-infected [lymphoblastic cell (LCL) and EBV-infected BJAB (E-BJAB)] and uninfected (BJAB) B cell lymphoma cell lines. The libraries comprised 3,988 individual compounds, including 1,988 FDA-approved small-molecule drugs and 2,000 natural products. We treated LCL, E-BJAB, and BJAB cells with a final concentration of 100 nM each compound for 72 h and counted the surviving cells by adding CellTiter-GloR to detect the ATP content. We selected compounds representing 0.8% (in the E-BJAB group) and 1.6% (in the LCL group) of libraries, which induced cytotoxicity in >50% of E-BJAB/LCL cells and also over 2-fold activity than that in BJAB cells (Figure 1A). Interestingly, most of the selected compounds (64% in LCL/BJAB and 70.6% in E-BJAB/BJAB) in the two groups were shown the effects of antitumor (39.7%, 32.4%), antibacterial (7.9%, 17.6%), antioxidant (7.9%, 8.8%), receptor antagonist (4.8%, 5.9%), and immunosuppressor (3.2%, 5.9%) (Figure 1B). In contrast, histone deacetylase inhibitor (14.3%), anti-malaria (6.4%), anti-angiogenic (4.8%), and Ca-antagonist (3.2%) appeared exclusively in the LCL/BJAB group, whereas the presence of hormone (11.8%) and nucleoside (11.8%) was noticeable in the E-BJAB/BJAB group.

To further screen compounds that target EBV-positive cells and have low toxicity to EBV-negative cells, we set up viability of EBV-uninfected cells >50% as an additional criterion for primary screening. Based on this standard, the secondary screening of selected compounds was performed, and we obtained a total of 31 (22 in the LCL/BJAB and 12 in the E-BJAB/BJAB, with three overlaps) types of effective compounds (Figure S1A). Among them, except for receptor antagonists, antitumor (32%, 23%), antibacterial (14%, 23%), antioxidant (9%, 15%), and immunosuppressor (4.5%, 8%) compounds remained in both groups, whereas histone deacetylase inhibitor (9%) and antimalaria (4.5%) only presented in the LCL/BJAB group (Figure S1B). Intriguingly, many of these have been documented to be associated with EBV infection or EBV-related cancers. For example, BAY1 is an inhibitor of the multifunctional transcription factor NF-κB, and has been shown to inhibit the growth of EBV-positive gastric cancer cells *in vitro*.[15] EBV can induce the expression of KLF14 by targeting the E2F-Rb-HDAC complex in latent infection, which could be blocked by histone deacetylase inhibitors (HDACI).[16] Moreover, the head shock protein 90 inhibitor BIIB021 (BIIB) exerts an inhibitory effect on EBV-associated T and NK lymphoma by inducing apoptosis or cell-cycle arrest.[17] Additionally, nocodazole (Noco) and MTH1 inhibitors induce the expression of two lytic proteins (Zta and EA-D) and the apoptosis of EBV-infected cancer cells.[18,19] These results confirm that our drug screening system targeting EBV-infected cells is reliable.

From the 31 qualified compounds obtained in the preliminary screening, we selected 11 compounds, including thiostrepton (Thio), adenine (Aden), adenine hydrochloride (AdeH), adenine sulfate (AdeS), acipimox (Acip), amlodipine besylate (AmlB), chlorothiazide (Chlo), cetrimonium bromide (CetB), celastrol (Cela), mirabex (Mira), and ginkgolide B (GinB), which have not been reported to associate with EBV or EBV-related tumors, for further verification.

CetB selectively inhibits the proliferation of diverse EBV-latently infected B lymphoma cell lines

To further verify the specific inhibition efficacy of these 11 compounds on EBV latently infected cells, we detected their cytotoxicity within effective and reasonable concentrations using another pair of EBV-infected and -uninfected B lymphoma cell lines, BL41-B95.8 vs. BL41, with the same genotype background. As shown in Figure 2, except for Thio and Cela, the remaining nine compounds presented higher inhibitory activity in the BL41-B95.8 cells than that in the BL41 cells. Among them, CetB is an interesting candidate that could be used for specific targeting of EBV latently infected cells because it presents significantly stronger inhibitory activity in EBV latently infected cells than in uninfected cells (IC50: 4.01 vs. 23.0 μM).

To further determine whether CetB can broadly and specifically inhibit the proliferation of EBV latently infected cells *in vitro*, we treated an equal quantity of four pairs of EBV latently infected and uninfected B lymphoma cell lines, including LCL/BJAB, BL41-B95.8/BL41, DG75-EBV/DG75, and Akata-EBV/Akata, in the presence and absence of different concentrations of CetB at different time points, and observed the cell number every day for 5 days. Interestingly, with DMSO as an internal control and using Thio and Cela (both of which have been previously reported to have strong antioxidant effect[20]) as two parallel controls (at a concentration of 0.5 μM), CetB consistently displayed a significantly high inhibitory effect on the proliferation of various EBV-positive cell lines compared to EBV-negative cell lines (Figure 3). Unexpectedly, the

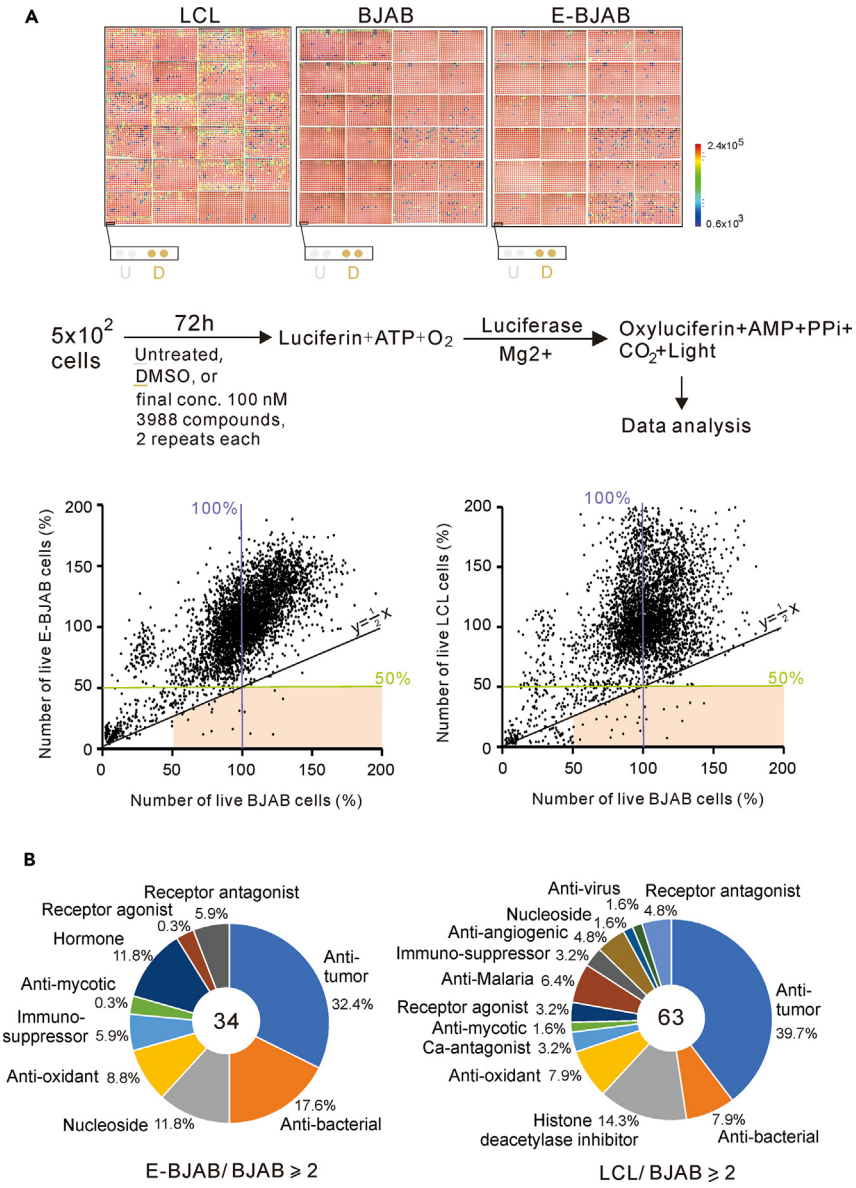

Figure 1. Identification of small molecules that induce cytotoxicity in EBV-infected but not uninfected B lymphoma cells

(A) LCL, E-BJAB, and BJAB B lymphoma cells were treated with libraries of 3,988 compounds from the FDA-approved and nature product collection. Cells were seeded in a 384-well plate with 50 μL of sample (0.5 × 10^3 cells) per well, before treating with 100 nM (final concentration) of each compound for 72 h. The ATP content was detected with CellTiter-GloR, and the proportion of live cells was counted. *Top panels*, red to purple indicates high to low fluorescence intensity, which in turn means high to low cell viability. *Middle panels,* streamlined workflow for high-throughput screening of small-molecule compounds against EBV-infected cancer cells. *Bottom panels*, the results were normalized using DMSO as a parallel negative control (standardized at 100% of live cells). The green lines are cutoff thresholds set at 50% of live cells for LCL or E-BJAB cells. Ninety-four compounds (2.4% of all compounds) shown in the orange square were selected from the initial screening.

(B) Group analysis of the biological functions of the 94 (three overlaps) compounds with ≥ 2-fold inhibitory efficiency from (A). The results are presented in percentage.

inhibitory effect of Cela on the proliferation of the EBV-negative cell lines BJAB and BL41 was much stronger than that of the EBV-positive cell lines LCL and BL41-B95.8, which is consistent with the lower cell viability of EBV-negative cells shown in Figure 2.

CetB selectively inhibits colony formation and tumor growth of EBV-infected B lymphoma cells *in vitro and in vivo*

Next, to examine the inhibitory efficacy of CetB for the treatment of EBV-related tumors *in vivo*, and considering Cela as an antioxidant compound is a potential promising strategy for treating EBV-infected cells as previous reports,[20–22] a xenograft mouse model was

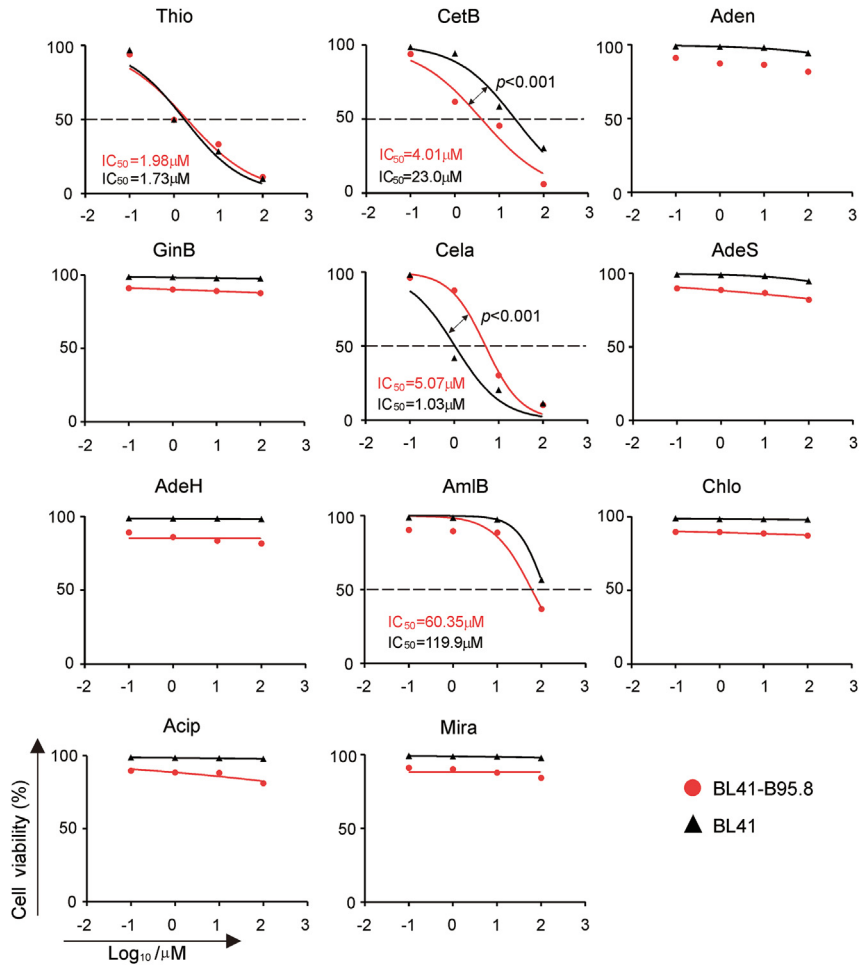

Figure 2. Cytotoxicity of 11 compounds on EBV-infected and -uninfected B lymphoma cells

EBV-infected BL41-B95.8 and uninfected BL41 cells were treated with 11 compounds selected from Figure S1A at different dosages (0, 0.1, 1, 10, and 100 μM) for 72 h, and the cell viability was measured using a live cell counter. The IC50 (μM) values of some compounds were calculated and shown.

created by engrafting B lymphoma LCL-Luc cells into non-obese diabetic/severe combined immunodeficiency (NOD/SCID) mice. On day 8 post engraftment, live bioluminescence imaging was performed to detect tumor signals within each mouse (Figure 4A, middle panels). Mice exhibiting similar intensities of tumor signals were randomly separated into groups treated with CetB (5 mg/kg), Cela (3 mg/kg), or both (CetB, 2.5 mg/kg and Cela 1.5 mg/kg) via intraperitoneal administration, with phosphate buffered saline (PBS) and DMSO used as parallel controls. After treatment with PBS/DMSO, CetB, or Cela, mice began gaining weight as early as 1 week due to tumor development. Mice treated with CetB maintained a relatively reduced weight, whereas those treated with Cela experienced abnormal weight loss (Figure 4B), suggesting that Cela has a side effect of toxicity that cannot be ignored. Interestingly, the inhibitory effect on the proliferation of LCL cells in mice in the CetB-only group was more than 2-fold that in the PBS/DMSO control group, and CetB significantly prolonged the survival period of mice within 40 days, without obvious side effects (Figure 4C). In contrast, although the inhibitory effect of both the Cela-only and CetB-Cela-combined groups on the proliferation of LCL cells in mice was approximately 5-fold greater than that of the PBS/DMSO control group, showing a greater tumor inhibitory effect, Cela showed significant toxicity in that the mice began to die earlier, the survival period of the five mice was much shorter than that of other groups, and the weight of the mice decreased abnormally.

To further confirm the selective effect of CetB on EBV-latently infected cells, we firstly performed the colony formation assays *in vitro* in the presence or absence of CetB treatment by using two pairs of EBV-infected and uninfected B lymphoma cell lines including Akata vs. Akata-EBV and BL41 vs. BL41-B95.8. The results showed that CetB significantly reduced the colony formation of EBV-latently infected Akata-EBV and BL41-B95.8 instead of uninfected Akata and BL41 cells (Figure 5A). In the xenograft mouse model *in vivo*, we also observed that CetB dramatically reduced the tumor growth of BL41-B95.8 cells, but not BL41 cells (Figure 5B), indicating that CetB selectively inhibits tumor growth of EBV-infected B lymphoma cells.

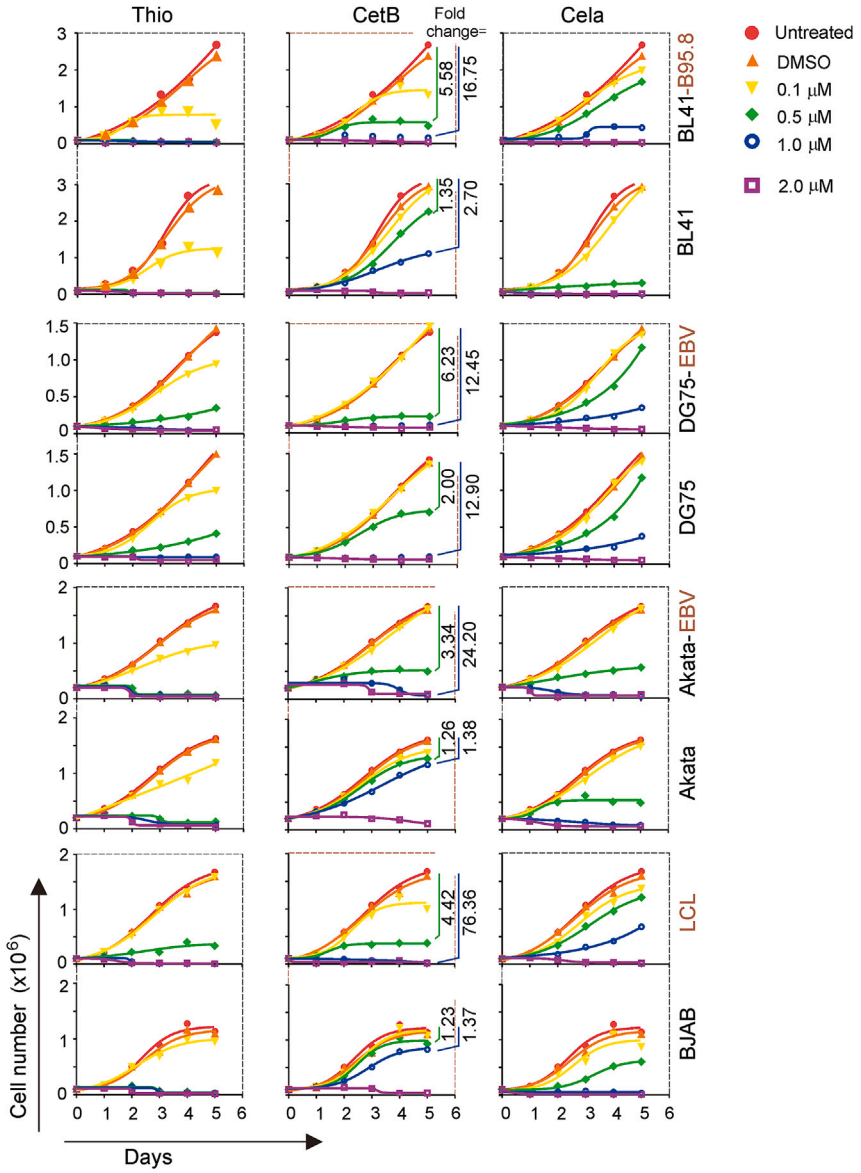

Figure 3. Inhibitory effects of three compounds on the proliferation of EBV-infected and -uninfected B lymphoma cells

The EBV-infected (BL41-B95.8, DG75-EBV, Akata-EBV, and LCL) and uninfected (BL41, DG75, Akata, and BJAB) B lymphoma cells were individually treated with three compounds (Thio, CetB, and Cela) selected from Figure 3 at different dosages (0, 0.1, 0.5, 1, and 2 μM) for 0, 1, 2, 3, 4, and 5 days. DMSO was used as a parallel control. The cell number was quantified using live cell counter.

CetB reduces EBNA1 protein stability and selectively induces G1 arrest and early apoptosis of EBV-infected B lymphoma cells without activating lytic replication

To further investigate how CetB selectively targets and kills EBV latently infected cells, we next conducted cell viability analysis of these four pairs of EBV-positive and -negative B lymphoma cell lines with different concentrations of CetB treatment for 48 h using CCK-8 staining. In agreement with the findings shown in Figure 3, we observed that the EBV-infected LCL, E-BJAB, Akata-EBV, DG75-EBV, and BL41-B95.8 cells were much more sensitive to CetB than the EBV-uninfected BJAB, Akata, DG75, and BL41 cells (Figure 6A). Furthermore, flow cytometric cell cycle analysis revealed that CetB consistently enhanced G1 phase arrest of EBV-positive BL41-B95.8 and Akata-EBV cell lines compared to the EBV-negative BL41 and Akata cell lines (Figure 6B). Consistently, we observed that early apoptosis was dramatically induced by CetB in EBV-positive cells but not EBV-negative cells (Figure 6C).

To determine whether the selective inhibitory effect of CetB on EBV-latently infected cells was due to the reactivation of EBV lytic replication, we next performed immunoblotting and virion particle production experiments in both LCL and BL41-B95.8 cells individually treated

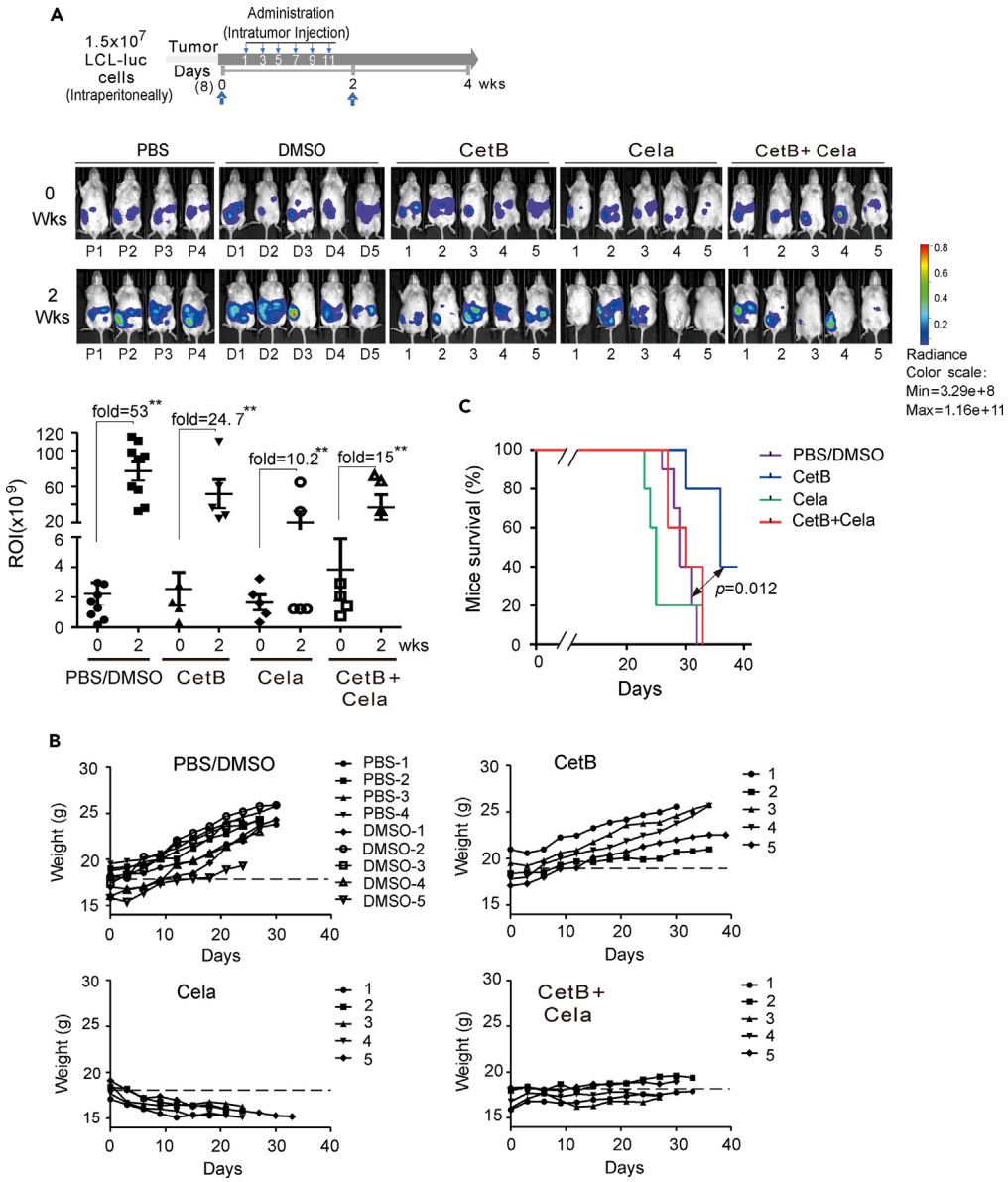

Figure 4. CetB significantly reduces EBV-infected B cell lymphoma growth *in vivo*

(A) Schematic diagram of NOD/SCID mice engrafted intraperitoneally with 15 million EBV-infected LCL-Luc cells on day 8 (week 0) and treated with PBS, DMSO, CetB (5 mg/kg), Cela (3 mg/kg), or combined (2.5 mg/kg CetB and 1.5 mg/kg Cela) by intratumor injection every other day for 1.5 weeks. *Middle panels*, the tumor burden of NOD/SCID mice was analyzed by luminescence assay at weeks 0 and 2. *Bottom panels*, luminescent signals were quantified and presented as the region of interest (ROI) signal intensity (total radiant efficiency [p/s]/[microwatt per cm^2]).

(B) Weights of NOD/SCID mice engrafted intraperitoneally with LCL-Luc cells for 8 days and then treated with or without CetB/Cela from (A) were monitored every 3 days for 5 weeks.

(C) Total percentage of mouse survival in each group from (A). The significant difference of *p* value between PBS/DMSO and CetB groups was calculated and shown in the figure.

with CetB. The results showed that along with the increased cell cytotoxicity of higher concentrations of CetB treatment, the production of viral particles in the culture supernatant was reduced (Figure 6D). Moreover, consistent with these observations, we did not observe a dramatic increase in the expression of ZTA after treatment with an increased concentration of CetB, whereas the expression of EBNA1 (the latent key antigen) was gradually reduced, along with increase of PARP1 cleavage (Figure 6E). In contrast, the protein level of LMP1 (another viral latent antigen) did not change upon the CetB treatment (Figure 6E). These results indicate that the activity of CetB selectively induced cytotoxicity in EBV-infected B lymphoma cells, probably due to targeting the key latent antigen EBNA1, instead of inducing the reactivation of lytic replication.

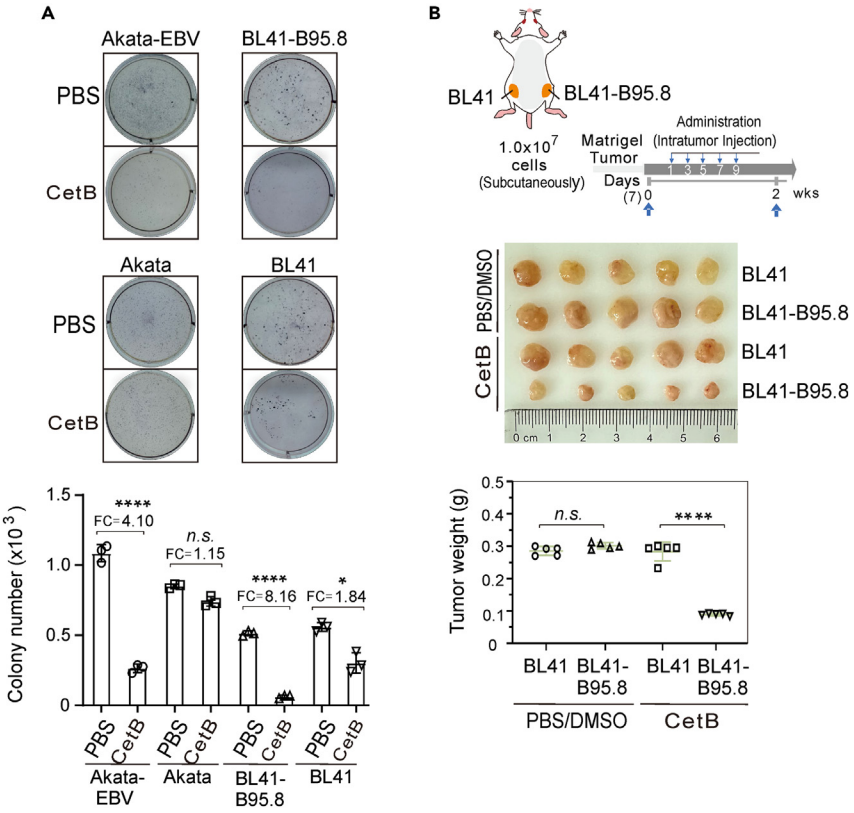

Figure 5. CetB selectively reduces colony formation and tumor growth of EBV-infected B lymphoma cells *in vitro* and *in vivo*

(A) CetB reduces the colony formation of EBV-infected B lymphoma cell lines *in vitro*. Equal amounts (5 ×10^4) of BL41, BL41-B95.8 (EBV), Akata, and Akata-EBV cells were individually inoculated and treated with or without CetB (0.5 μM) and subjected to colony formation assays as indicated. The cells were fixed 2 weeks later and stained with NBT to determine colony number. The colony number were quantified and shown at the bottom panel.

(B) CetB selectively inhibits tumor growth of EBV-infected B lymphoma cells *in vivo*. Schematic diagram of BABL/c-nu mice engrafted subcutaneously with 10 million BL41 or BL41-B95.8 cells on day 7 (week 0) and treated with PBS, DMSO, or CetB (5 mg/kg) by intratumor injection every other day for 9 days. *Middle panels*, the tumor burden of ten BABL/c-nu mice from top panels were sacrificed and isolated for tumor analysis at 2 weeks later. The tumor weights were quantified and shown at the bottom panels. ****$p < 0.001$. n.s., non-significant.

To further elucidate how the expression of EBNA1 is downregulated by CetB, LCL cells treated with different concentrations of CetB in the presence or absence of caspase 3/7 inhibitor Z-DEVD-FMK were individually subjected to immunoblotting with EBNA1 antibodies. Interestingly, the results showed that caspase 3/7 inhibitor efficiently blocked the CetB-induced reduction of EBNA1 protein level (Figure 7A). With the treatment of cycloheximide, the results further showed that CetB reduced the protein stability of EBNA1 (Figure 7B), while no influence on the EBNA1 transcripts (Figure 7C).

CetB selectively inhibits the proliferation of EBV- but not KSHV (Kaposi's sarcoma-associated Herpesvirus)-infected cells

Considering that CetB is screened mainly based on different EBV-infected B lymphoma cell lines, we next sought to determine whether CetB could selectively inhibit the proliferation of EBV-infected cells independent of cell type. To this end, we attempted to determine the effect of CetB on EBV-infected and -uninfected NPC cell lines using C666-1 and 5-8F, with KSHV (another herpesvirus with highly homologous to EBV[23])-infected B lymphoma cell lines K-BJAB and BCBL1, as well as EBV and KSHV double-positive B lymphoma cell lines JSC1 and BC1 used as parallel controls. Intriguingly, the results confirmed that the proliferation of the EBV-positive C666-1 cells was inhibited significantly more than that of the EBV-negative 5-8F cells when the concentration of CetB reached 0.5 μM (Figure S2, top panels). Moreover, with an increase in the concentration of CetB, the selective inhibitory effect on proliferation became more obvious (Figure S2, top panels). In contrast, CetB had no selective effect on the inhibition of KSHV-infected B lymphoma BCBL1 or K-BJAB cells when compared to BJAB cells (Figure S2, middle panels), while CetB presented moderate inhibitory effects on both EBV and KSHV double-positive B lymphoma JSC1 and BC1 cells at the concentration of 1.0 μM (Figure S2, bottom panels). These results indicate that CetB could broadly and selectively inhibit the proliferation of EBV (but not KSHV)-infected host cells, regardless of whether they were lymphoma or nasopharyngeal carcinoma cells, and co-infection with KSHV or not.

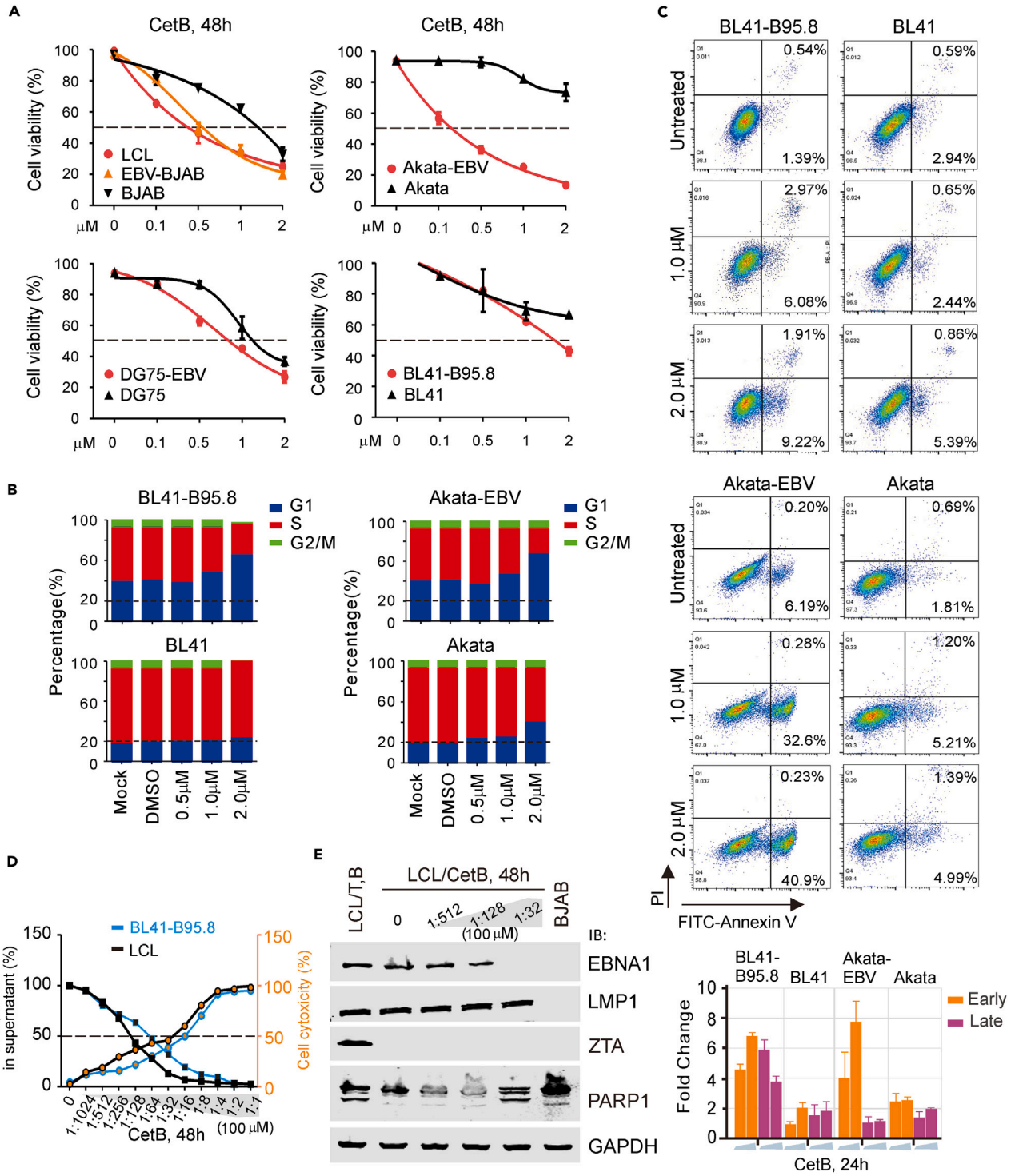

Figure 6. CetB selectively induces G1-arrest and early apoptosis of EBV-infected B lymphoma cells without activation of lytic replication

(A) Cytotoxicity of CetB on EBV-infected (BL41-B95.8, DG75-EBV, Akata-EBV, and LCL) and -uninfected (BL41, DG75, Akata, and BJAB) B lymphoma cell lines. Cells (5×10^3) were seeded in a 96-well plate (100 μL per well) and treated with different concentrations of CetB, as indicated, for 48 h. The percentage of cell viability was measured by CCK-8 staining, and compared with that of the untreated group.

(B) CetB selectively induces G1 arrest of EBV-infected B lymphoma cells. Cells treated with 0.5, 1, or 2 μM CetB for 24 h, as indicated, were analyzed by flow cytometry after propidium iodide staining. Untreated (mock) and DMSO were used as parallel controls. The percentages of G1, S, and G2/M populations were quantified from triplicate experiments.

Figure 6. *Continued*

(C) CetB dramatically enhanced early apoptosis of EBV-infected but not -uninfected B lymphoma cells. Cells treated with or without 1 or 2 μM CetB for 24 h, as indicated, were analyzed by flow cytometry after FITC-Annexin V and propidium iodide staining. The percentages of early apoptotic cells (positive for only Annexin V) or late apoptotic cells (positive for only PI) are highlighted. The relative fold change of early and late apoptosis of each cell line after CetB treatment is shown in the bottom panel.

(D) CetB induces cytotoxicity and blocks production of EBV viral particles. LCL or BL41-B95.8 cells (5×10^3) were seeded in a 96-well plate (100 μL per well) and treated with different concentrations of CetB, as indicated, for 48 h, with three replicate wells per experimental group. The CetB-induced cell cytotoxicity was measured by a live cell counter and presented as the relative percentage compared to the untreated group. The viral particles in culture supernatant were detected by quantitative PCR, and are presented as the relative percentage compared to the untreated group.

(E) CetB reduced the expression of EBNA1 without activating ZTA expression. Immunoblotting results of LCL cells treated with CetB from (C). The LCL cells treated with TPA and sodium butyrate (T and B), and BJAB cells were used as controls.

CetB selectively inhibits the *in vitro* proliferation of clinical EBV-infected cells derived from patients with B lymphoma

Considering that CetB showed a promising selective inhibitory activity on EBV-infected cell lines, we next wondered whether CetB has the same effect on clinical EBV-infected cells derived from patients with B lymphoma. To investigate this, we first generated five EBV-infected BJAB cell lines by infecting them with clinical EBV viral particles (individually isolated from the peripheral blood plasma of five patients [P1–P5] with hemophagocytic syndrome) for 7 days (Figure 8A, top panels, the EBV infection rate were verified and quantified by immunofluorescent staining with EBNA1 and shown in both bottom panel; Figure S3), before performing *in vitro* proliferation analysis with different concentrations of CetB. The results showed that the inhibitory efficacy of CetB (1 μM) on clinical EBV-infected BJAB cell lines of P3, P4, or P5 was almost twice that observed on uninfected BJAB cells (Figure 8A, middle panels). In contrast, the inhibitory effect of CetB on clinical wild-type EBV-BJAB generated from P1 and P2 showed moderate inhibitory activity. However, when the concentration of CetB reached 2 μM, there was no significant difference in the inhibition of proliferation between the clinical wild-type EBV-BJAB cells and its parental BJAB cells.

We next sought to determine whether the selective inhibitory effect of CetB on clinical wild-type EBV-infected cells has the potential to treat EBV-positive B lymphoma patients. We selected eight patients with DLBCL with or without EBV infection and harvested and treated their peripheral blood mononuclear cells (PBMCs) with different concentrations of CetB *in vitro* for 48 h. The results showed that the inhibitory effects of PBMCs on EBV-positive patients were significantly greater than those on EBV-negative patients when the concentration of CetB reached 2 μM (Figure 8B). Consistently, using CD3 and CD20 staining for T cells and B cells, respectively, we found that the B cell population from EBV-positive, but not EBV-negative patients with DLBCL was significantly inhibited by increasing concentrations of CetB (Figure 8C).

Taken together, we have identified CetB as a promising candidate for treating patients with EBV-infected B lymphoma. As CetB displays a potent selectively inhibitory effect on EBV-infected cells by targeting EBV latent infection, it would be great interesting to conduct advanced preclinical and clinical trials for its use in the treatment of EBV-associated cancers.

DISCUSSION

EBV is an oncogenic virus that is associated with many human malignancies.[24–26] Many studies have explored how EBV establishes life-long latency in the human host and is adept at evading host innate and adaptive immune responses.[24,27,28] However, there is currently no specific and efficient therapy for EBV-associated cancers, although there are many experimental and empirical treatments for EBV-associated lymphoma. For example, antiviral compounds that inhibit viral replication have been shown to have no significant effect on tumors,[29] largely because the viral thymidine kinase, as a target of nucleoside-type antiviral agents (ganciclovir and acyclovir), is expressed only in the EBV lytic phase.[30] Moreover, ESTs (expressed sequence tags), as an adoptive T cell therapy that can be generated from allogeneic, autologous, or third-party donors, target EBV antigens that are presented on the cell surface by major histocompatibility complex molecules.[31] However, ongoing immunosuppression, the time consuming process to generate ESTs, and the possibility of seronegativity render this approach challenging for broader application.[32] Therefore, the development of more effective therapeutic strategies by targeting EBV latent infection is urgently required.

To ensure the effective identification of small-molecule compounds specifically targeting EBV-infected cells, we selected 1,988 FDA-approved small-molecule compounds and 2,000 natural products for high-throughput screening using several pairs of EBV-infected and -uninfected B lymphoblastic cell lines with the same genotype background to enhance the possibility of identifying compounds with specific inhibition of EBV-infected cells. Interestingly, in the initial screening, 31 compounds were found to significantly inhibit the proliferation of EBV-positive, but not negative B lymphoma cells *in vitro*. Subsequently, three effective candidate compounds were confirmed using additional pairs of EBV-positive and -negative cell lines. Among them, CetB is a cationic quaternary ammonium salt surfactant, which is one of the components of the topical disinfectant cetrimide. CetB has been shown to be involved in suppressing the TGF-β-mediated mesenchymal phenotype and may be an effective drug to control the migration and invasion of HCC.[33] CetB has also been previously reported as a potential therapeutic agent for head and neck tumors.[34] In contrast, Cela is a natural product with a variety of biological activities and has strong antioxidant, anticancer angiogenesis, and anti-rheumatoid effects. Through the re-screening identification of multiple pairs of EBV-positive and -negative cell lines, CetB consistently presents as a promising candidate for selective inhibition of the proliferation of EBV latently infected cancer cells.

In this study, CetB was demonstrated to exclusively inhibit not only the proliferation of B lymphoma cells infected with the clinical EBV strain (isolated from patients with hemophagocytic syndrome), but also PBMCs from patients with EBV-positive lymphoma. Moreover, CetB treatment could dramatically induce regression of EBV-positive B lymphoma in a xenograft mouse model and significantly prolong

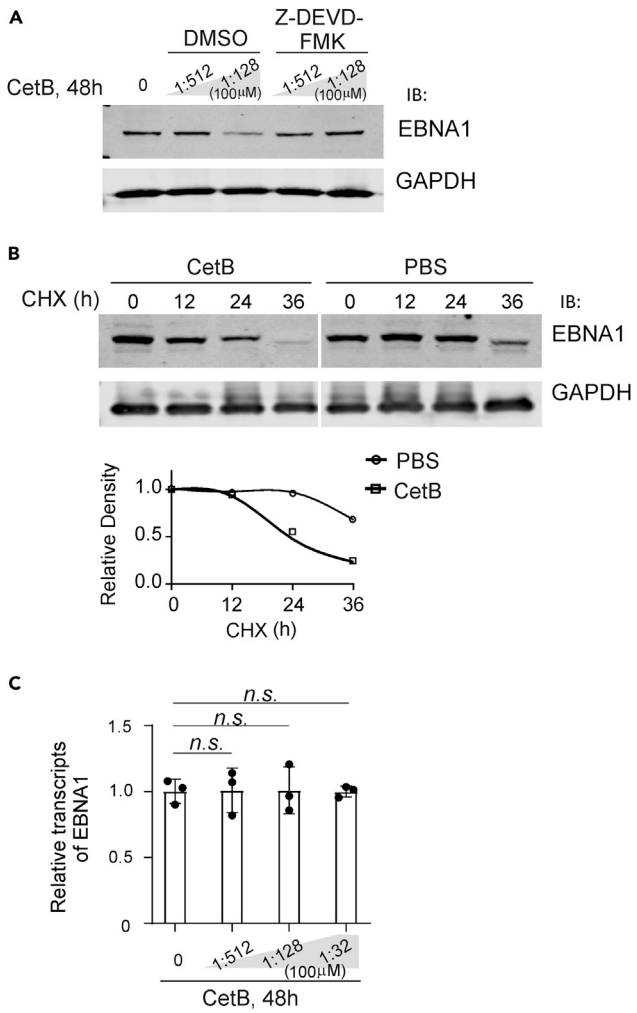

Figure 7. CetB impairs the protein stability of EBNA1 not its transcripts in EBV-infected LCL cells

(A) CetB induces caspase -mediated EBNA1 degradation. LCL cells were treated with different concentrations of CetB for 48 h in the presence or absence of caspase 3/7 inhibitor (Z-DEVD-FMK, 200 μg/mL) as indicated in the figure, followed by immunoblotting with EBNA1 antibody. GAPDH was used as an internal control.

(B) CetB reduces protein stability of EBNA1. LCL cells treated with or without CetB (0.19μM) for 6 h, were subjected to cycloheximide (CHX, 200 μg/mL) treatment for the indicated time before harvesting and lysing for immunoblotting (IB). The relative density of EBNA1 was quantified and shown at the bottom panel.

(C) CetB does not impair the transcripts of EBNA1. LCL cells treated with different concentrations of CetB for 48 h were subjected to quantitative PCR analysis for EBNA1 transcripts. GAPDH was used as an internal control. n.s., non-significant.

the survival of tumor-bearing mice. CetB also exhibited an inhibitory effect exclusively on the proliferation of EBV-positive not negative nasopharyngeal carcinoma cell lines *in vitro*, whereas there was almost no inhibitory effect on the proliferation of KSHV-positive cell lines, indicating that CetB may be an ideal candidate for selectively treating EBV-positive cancers. To further explore why CetB can selectively inhibit EBV latently infected, but not uninfected cancer cells, we examined the effects of CetB on the cell cycle and viral life cycle. Interestingly, the results showed that CetB dramatically inhibited the expression of the EBV latent antigen EBNA1 without reactivating lytic replication, which in turn, reduced the production of EBV viral progeny particles, possibly due to inducing G1 arrest and early apoptosis of host cells. However, the more detailed mechanisms underlying the targeting effects of CetB on EBV latently infected cells require further investigation.

In summary, we identified CetB as a potential promising therapeutic agent for treating EBV latently infected cells and provided evidence for the development of comprehensive and effective treatment strategies against EBV-associated cancers.

Limitations of the study

The effectivity and feasibility of CetB remains to be further demonstrated in the clinical treatment for patients with EBV-associated cancers, although we have found CetB is a potential therapeutic drug for selectively inhibiting EBV-infected cell growth in cell lines and murine xenograft-tumor model.

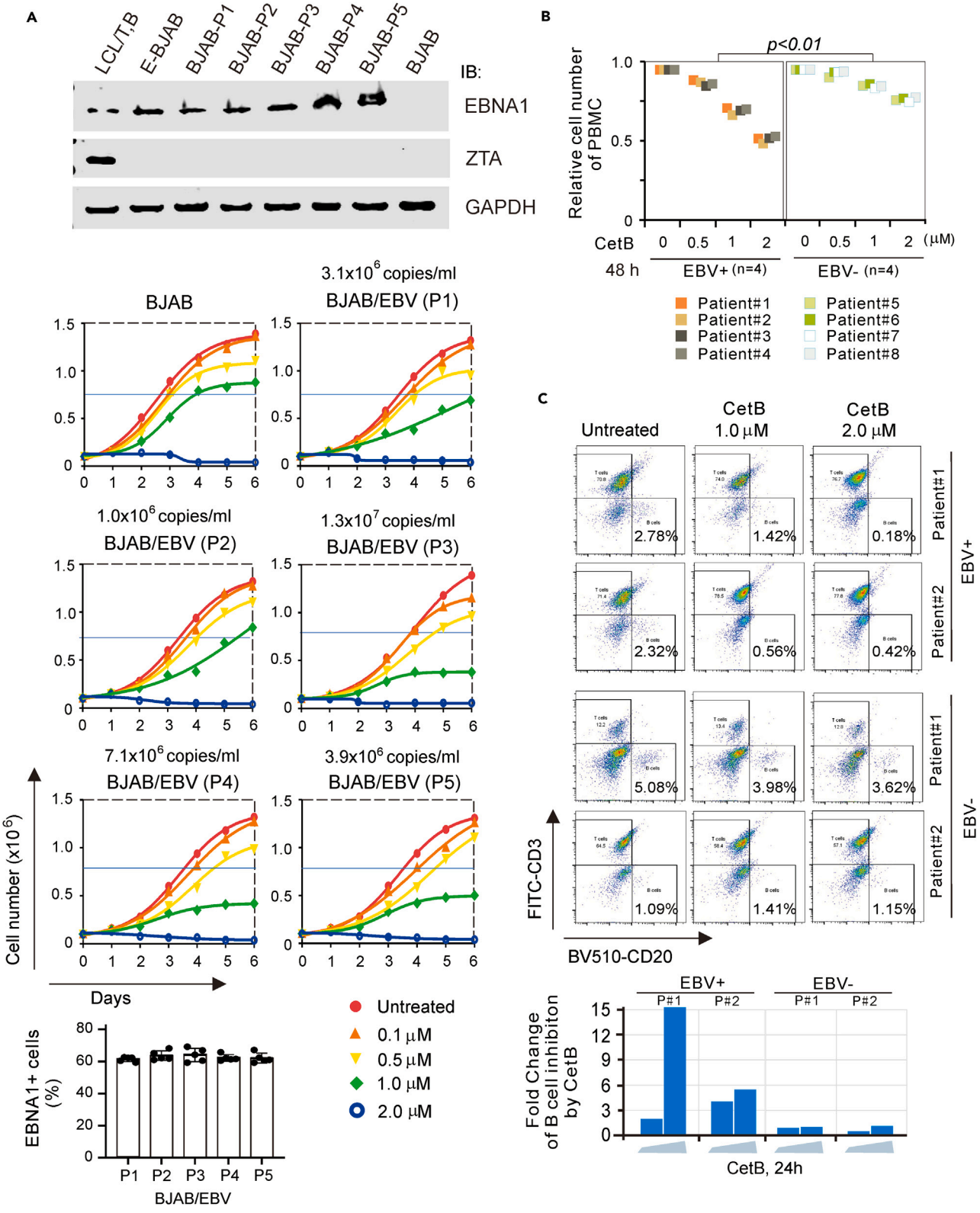
A
LCL/T;B
E-BJAB
BJAB-P1
BJAB-P2
BJAB-P3
BJAB-P4
BJAB-P5
BJAB
IB:
EBNA1
ZTA
GAPDH
B
p<0.01
Relative cell number of PBMC
CetB
48 h
EBV+ (n=4)
EBV- (n=4)
(μM)
Patient#1
Patient#2
Patient#3
Patient#4
Patient#5
Patient#6
Patient#7
Patient#8
BJAB
3.1x10^6 copies/ml
BJAB/EBV (P1)
1.0x10^6 copies/ml
BJAB/EBV (P2)
1.3x10^7 copies/ml
BJAB/EBV (P3)
7.1x10^6 copies/ml
BJAB/EBV (P4)
3.9x10^6 copies/ml
BJAB/EBV (P5)
Cell number (x10^6)
Days
Untreated
0.1 μM
0.5 μM
1.0 μM
2.0 μM
EBNA1+ cells (%)
P1 P2 P3 P4 P5
BJAB/EBV
C
Untreated
CetB 1.0 μM
CetB 2.0 μM
2.78%
1.42%
0.18%
2.32%
0.56%
0.42%
5.08%
3.98%
3.62%
1.09%
1.41%
1.15%
Patient#1
Patient#2
EBV+
EBV-
FITC-CD3
BV510-CD20
EBV+
EBV-
P#1 P#2 P#1 P#2
Fold Change of B cell inhibiton by CetB
CetB, 24h

Figure 8. CetB selectively inhibits the *in vitro* proliferation of EBV-infected cells derived from patients with B cell lymphoma

(A) Inhibitory effects of CetB on the proliferation of B lymphoma cells infected with wild-type EBV strain. *Top panels*, the immunoblotting analysis of BJAB cells infected with wild-type EBV from the plasma of patients with hemophagocytic syndrome. The whole cell lysates extracted at 7 days post infection were subjected to immunoblotting, as indicated. *Middle panels*, the BJAB cells infected with wild-type EBV strains from the *top panel* were individually treated with CetB at different dosages (0, 0.1, 0.5, 1, and 2 μM) for 0, 1, 2, 3, 4, 5, and 6 days. The cell number was quantified using a live cell counter. The EBV viral copy number per mL in the plasma of each patient (P1, P2, P3, P4, and P5) is shown in the top panels. The percentage of BJAB cells with EBV infection were quantified by EBNA1-positive staining and shown at the bottom panel. The representative immunofluorescent staining of EBNA1 was shown in the Figure S3. The LCL cells treated with TPA and sodium butyrate (T and B), and BJAB cells were used as controls.

(B) CetB dramatically reduced the viability of PBMCs from patients with EBV-positive B cell lymphoma. PBMCs (1 million per mL) from patients with EBV-positive (P#1 to P#4) and negative (P#5 to P#8) diffuse large B cell lymphoma (DLBCL) were individually cultured in a 6-well plate and treated with different final concentrations of CetB (0, 0.5, 1, and 2 μM) for 48 h, before counting with a live cell counter to determine the viability. The presented data are from duplicated experiments.

(C) CetB selectively inhibits the B cell but not T cell population in PBMCs from patients with EBV-positive B cell lymphoma. PBMCs from patients with EBV-positive and -negative diffuse large B cell lymphoma were subjected to CetB treatment for 24 h, followed by flow cytometry analysis with FITC-CD3 and BV510-CD20 staining for T cells and B cells, respectively. The relative fold change of the B cell population in each patient after CetB treatment is shown in the bottom panel.

STAR★METHODS

Detailed methods are provided in the online version of this paper and include the following:

- KEY RESOURCES TABLE
- RESOURCE AVAILABILITY
  - Lead contact
  - Materials availability
  - Data and code availability
- EXPERIMENTAL MODEL AND STUDY PARTICIPANT DETAILS
  - Human participants
  - Cell lines
  - Animals
- METHOD DETAILS
  - High-throughput screening
  - Cell proliferation assay
  - Cytotoxicity assay *in vitro*
  - Quantitation of EBV episome DNA
  - Establishment of clinical EBV-infected B-lymphoma cell lines
  - Cell cycle and apoptosis assay
  - Flow cytometry analysis of human PBMC
  - Immunoblotting assay
  - Immunofluorescence
  - Soft agar colony formation
  - Quantitative PCR
  - Tumor xenograft
- QUANTIFICATION AND STATISTICAL ANALYSIS

SUPPLEMENTAL INFORMATION

Supplemental information can be found online at https://doi.org/10.1016/j.isci.2024.110581.

ACKNOWLEDGMENTS

We thank members of the Cai laboratory for technical assistance and helpful discussions, and the staff (Shen Cai, Xiao Guo, and Yao Wang) from core facility of microbiology and parasitology of SHMC for technical supports. This work was supported by the National Key Research and Development Program of China (2023YFC2306702 and 2021YFA130080), National Natural Science Foundation of China (32120103001, 82372242, 82272324, and 82102386), Program of Shanghai Academic Research Leader (22XD1403000), Shanghai Municipal Science and Technology Project (23JC1401302 and ZD2021CY001), and Jinan University and Institute Innovation Program (2020GXRC043). Q.C. is a scholar of New Century Excellent Talents in University of China and Oriental Talent Leader of Shanghai.

AUTHOR CONTRIBUTIONS

Y.L., F.W., and Q.C. designed the experiments, analyzed and organized data, and wrote the paper; Y.L., S.D., K.Z., and Y.Z. performed the experiments; Y.J. and D.Z. helped compounds screening and analysis; X.C., C.Z., and Y.W. provided technology and animal experiment support; K.Z. and Y. T. provided patient tissues samples and clinical analysis. All authors discussed the results and commented on the manuscript.

DECLARATION OF INTERESTS

The authors declare no competing interest.

Received: January 10, 2024
Revised: May 10, 2024
Accepted: July 22, 2024
Published: July 25, 2024

REFERENCES

1. Chiu, Y.F., and Sugden, B. (2016). Epstein-Barr Virus: The Path from Latent to Productive Infection. Annu. Rev. Virol. *3*, 359–372. https://doi.org/10.1146/annurev-virology-110615-042358.
2. Epstein, M.A., Achong, B.G., and Barr, Y.M. (1964). Virus particles in cultured lymphoblasts from burkitt's lymphoma. Lancet *1*, 702–703. https://doi.org/10.1016/s0140-6736(64)91524-7.
3. Ohga, S., Nomura, A., Takada, H., and Hara, T. (2002). Immunological aspects of Epstein-Barr virus infection. Crit. Rev. Oncol. Hematol. *44*, 203–215. https://doi.org/10.1016/s1040-8428(02)00112-9.
4. Thorley-Lawson, D.A., and Gross, A. (2004). Persistence of the Epstein-Barr virus and the origins of associated lymphomas. N. Engl. J. Med. *350*, 1328–1337. https://doi.org/10.1056/NEJMra032015.
5. Molyneux, E.M., Rochford, R., Griffin, B., Newton, R., Jackson, G., Menon, G., Harrison, C.J., Israels, T., and Bailey, S. (2012). Burkitt's lymphoma. Lancet *379*, 1234–1244.
6. Jones, K., Nourse, J.P., Keane, C., Crooks, P., Gottlieb, D., Ritchie, D.S., Gill, D., and Gandhi, M.K. (2012). Tumor-specific but not nonspecific cell-free circulating DNA can be used to monitor disease response in lymphoma. Am. J. Hematol. *87*, 258–265. https://doi.org/10.1002/ajh.22252.
7. Martinez, O.M. (2020). Biomarkers for PTLD diagnosis and therapies. Pediatr. Nephrol. *35*, 1173–1181. https://doi.org/10.1007/s00467-019-04284-w.
8. Kanakry, J.A., Li, H., Gellert, L.L., Lemas, M.V., Hsieh, W.S., Hong, F., Tan, K.L., Gascoyne, R.D., Gordon, L.I., Fisher, R.I., et al. (2013). Plasma Epstein-Barr virus DNA predicts outcome in advanced Hodgkin lymphoma: correlative analysis from a large North American cooperative group trial. Blood *121*, 3547–3553. https://doi.org/10.1182/blood-2012-09-454694.
9. Castillo, J.J., Beltran, B.E., Miranda, R.N., Young, K.H., Chavez, J.C., and Sotomayor, E.M. (2016). EBV-positive diffuse large B-cell lymphoma of the elderly: 2016 update on diagnosis, risk-stratification, and management. Am. J. Hematol. *91*, 529–537. https://doi.org/10.1002/ajh.24370.
10. Münz, C. (2019). Latency and lytic replication in Epstein-Barr virus-associated oncogenesis. Nat. Rev. Microbiol. *17*, 691–700. https://doi.org/10.1038/s41579-019-0249-7.
11. Qiu, J., Cosmopoulos, K., Pegtel, M., Hopmans, E., Murray, P., Middeldorp, J., Shapiro, M., and Thorley-Lawson, D.A. (2011). A novel persistence associated EBV miRNA expression profile is disrupted in neoplasia. PLoS Pathog. *7*, e1002193. https://doi.org/10.1371/journal.ppat.1002193.
12. Pagano, J.S., Whitehurst, C.B., and Andrei, G. (2018). Antiviral Drugs for EBV. Cancers *10*, 197. https://doi.org/10.3390/cancers10060197.
13. Gershburg, E., and Pagano, J.S. (2005). Epstein-Barr virus infections: prospects for treatment. J. Antimicrob. Chemother. *56*, 277–281. https://doi.org/10.1093/jac/dki240.
14. Kalinova, L., Indrakova, J., and Bachleda, P. (2009). Post-transplant lymphoproliferative disorder. Biomed. Pap. Med. Fac. Univ. Palacky Olomouc Czech. Repub. *153*, 251–257. https://doi.org/10.5507/bp.2009.043.
15. Zhang, Y., Liu, W., Zhang, W., Wang, W., Song, Y., Xiao, H., and Luo, B. (2019). Constitutive activation of the canonical NF-κB signaling pathway in EBV-associated gastric carcinoma. Virology *532*, 1–10. https://doi.org/10.1016/j.virol.2019.03.019.
16. Pei, Y., Wong, J.H.Y., Jha, H.C., Tian, T., Wei, Z., and Robertson, E.S. (2020). Epstein-Barr Virus Facilitates Expression of KLF14 by Regulating the Cooperative Binding of the E2F-Rb-HDAC Complex in Latent Infection. J. Virol. *94*, e01209-20. https://doi.org/10.1128/jvi.01209-20.
17. Suzuki, M., Takeda, T., Nakagawa, H., Iwata, S., Watanabe, T., Siddiquey, M.N.A., Goshima, F., Murata, T., Kawada, J.I., Ito, Y., et al. (2015). The heat shock protein 90 inhibitor BIIB021 suppresses the growth of T and natural killer cell lymphomas. Front. Microbiol. *6*, 280. https://doi.org/10.3389/fmicb.2015.00280.
18. Liu, Y.R., Huang, S.Y., Chen, J.Y., and Wang, L.H.C. (2013). Microtubule depolymerization activates the Epstein-Barr virus lytic cycle through protein kinase C pathways in nasopharyngeal carcinoma cells. J. Gen. Virol. *94*, 2750–2758. https://doi.org/10.1099/vir.0.058040-0.
19. Wang, J., Nagy, N., and Masucci, M.G. (2020). The Epstein-Barr virus nuclear antigen-1 upregulates the cellular antioxidant defense to enable B-cell growth transformation and immortalization. Oncogene *39*, 603–616. https://doi.org/10.1038/s41388-019-1003-3.
20. Gilardini Montani, M.S., Santarelli, R., Granato, M., Gonnella, R., Torrisi, M.R., Faggioni, A., and Cirone, M. (2019). EBV reduces autophagy, intracellular ROS and mitochondria to impair monocyte survival and differentiation. Autophagy *15*, 652–667. https://doi.org/10.1080/15548627.2018.1536530.
21. Wang, J., Nagy, N., and Masucci, M.G. (2020). The Epstein-Barr virus nuclear antigen-1 upregulates the cellular antioxidant defense to enable B-cell growth transformation and immortalization. Oncogene *39*, 2028. https://doi.org/10.1038/s41388-019-1066-1.
22. Hu, J., Li, Y., Li, H., Shi, F., Xie, L., Zhao, L., Tang, M., Luo, X., Jia, W., Fan, J., et al. (2020). Targeting Epstein-Barr virus oncoprotein LMP1-mediated high oxidative stress suppresses EBV lytic reactivation and sensitizes tumors to radiation therapy. Theranostics *10*, 11921–11937. https://doi.org/10.7150/thno.46006.
23. Ding, L., Zhu, Q., Zhou, F., Tan, H., Xu, W., Pan, C., Zhu, C., Wang, Y., Zhang, H., Fu, W., et al. (2019). Identification of viral SIM-SUMO2-interaction inhibitors for treating primary effusion lymphoma. PLoS Pathog. *15*, e1008174. https://doi.org/10.1371/journal.ppat.1008174.
24. Damania, B., Kenney, S.C., and Raab-Traub, N. (2022). Epstein-Barr virus: Biology and clinical disease. Cell *185*, 3652–3670. https://doi.org/10.1016/j.cell.2022.08.026.
25. Dharnidharka, V.R. (2018). Comprehensive review of post-organ transplant hematologic cancers. Am. J. Transplant. *18*, 537–549. https://doi.org/10.1111/ajt.14603.
26. Bourbon, E., Maucort-Boulch, D., Fontaine, J., Mauduit, C., Sesques, P., Safar, V., Ferrant, E., Golfier, C., Ghergus, D., Karlin, L., et al. (2021). Clinicopathological features and survival in EBV-positive diffuse large B-cell lymphoma not otherwise specified. Blood Adv. *5*, 3227–3239. https://doi.org/10.1182/bloodadvances.2021004515.
27. Singh, D.R., Nelson, S.E., Pawelski, A.S., Kansra, A.S., Fogarty, S.A., Bristol, J.A., Ohashi, M., Johannsen, E.C., and Kenney, S.C. (2023). Epstein-Barr virus LMP1 protein promotes proliferation and inhibits differentiation of epithelial cells via activation of YAP and TAZ. Proc. Natl. Acad. Sci. USA *120*, e2219755120. https://doi.org/10.1073/pnas.2219755120.
28. Albanese, M., Tagawa, T., Bouvet, M., Maliqi, L., Lutter, D., Hoser, J., Hastreiter, M., Hayes, M., Sugden, B., Martin, L., et al. (2016). Epstein-Barr virus microRNAs reduce immune surveillance by virus-specific CD8+ T cells. Proc. Natl. Acad. Sci. USA *113*, E6467–E6475. https://doi.org/10.1073/pnas.1605884113.
29. Bollard, C.M., Rooney, C.M., and Heslop, H.E. (2012). T-cell therapy in the treatment of post-transplant lymphoproliferative disease. Nat. Rev. Clin. Oncol. *9*, 510–519. https://doi.org/10.1038/nrclinonc.2012.111.
30. Perrine, S.P., Hermine, O., Small, T., Suarez, F., O'Reilly, R., Boulad, F., Fingeroth, J., Askin, M., Levy, A., Mentzer, S.J., et al. (2007). A phase 1/2 trial of arginine butyrate and ganciclovir in patients with Epstein-Barr virus-associated lymphoid malignancies. Blood *109*, 2571–2578. https://doi.org/10.1182/blood-2006-01-024703.
31. Toner, K., and Bollard, C.M. (2022). EBV+ lymphoproliferative diseases: opportunities for leveraging EBV as a therapeutic target. Blood *139*, 983–994. https://doi.org/10.1182/blood.2020005466.
32. Wistinghausen, B., Gross, T.G., and Bollard, C. (2013). Post-transplant lymphoproliferative disease in pediatric solid organ transplant recipients. Pediatr. Hematol. Oncol. *30*,

520–531. https://doi.org/10.3109/08880018.2013.798844.

33. Wu, T.K., Chen, C.H., Pan, Y.R., Hu, C.W., Huang, F.M., Liu, J.Y., and Lee, C.J. (2019). Cetrimonium Bromide Inhibits Cell Migration and Invasion of Human Hepatic SK-HEP-1 Cells Through Modulating the Canonical and Non-canonical TGF-β Signaling Pathways. Anticancer Res. *39*, 3621–3631. https://doi.org/10.21873/anticanres.13510.

34. Ito, E., Yip, K.W., Katz, D., Fonseca, S.B., Hedley, D.W., Chow, S., Xu, G.W., Wood, T.E., Bastianutto, C., Schimmer, A.D., et al. (2009). Potential use of cetrimonium bromide as an apoptosis-promoting anticancer agent for head and neck cancer. Mol. Pharmacol. *76*, 969–983. https://doi.org/10.1124/mol.109.055277.

35. Cai, Q.L., Knight, J.S., Verma, S.C., Zald, P., and Robertson, E.S. (2006). EC5S ubiquitin complex is recruited by KSHV latent antigen LANA for degradation of the VHL and p53 tumor suppressors. PLoS Pathog. *2*, e116.

36. Saha, A., Halder, S., Upadhyay, S.K., Lu, J., Kumar, P., Murakami, M., Cai, Q., and Robertson, E.S. (2011). Epstein-Barr virus nuclear antigen 3C facilitates G1-S transition by stabilizing and enhancing the function of cyclin D1. PLoS Pathog. *7*, e1001275.

37. Mo, X., Wei, F., Tong, Y., Ding, L., Zhu, Q., Du, S., Tan, F., Zhu, C., Wang, Y., Yu, Q., et al. (2018). Lactic Acid Downregulates Viral MicroRNA To Promote Epstein-Barr Virus-Immortalized B Lymphoblastic Cell Adhesion and Growth. J. Virol. *92*, e00033-18.

38. Mo, X., Du, S., Chen, X., Wang, Y., Liu, X., Zhang, C., Zhu, C., Ding, L., Li, Y., Tong, Y., et al. (2020). Lactate Induces Production of the $tRNA^{His}$ Half to Promote B-lymphoblastic Cell Proliferation. Mol. Ther. *28*, 2442–2457.

39. Han, X., Du, S., Chen, X., Min, X., Dong, Z., Wang, Y., Zhu, C., Wei, F., Gao, S., and Cai, Q. (2023). Lactate-mediated Fascin protrusions promote cell adhesion and migration in cervical cancer. Theranostics *13*, 2368–2383.

40. Zhu, Q., Ding, L., Zi, Z., Gao, S., Wang, C., Wang, Y., Zhu, C., Yuan, Z., Wei, F., and Cai, Q. (2019). Viral-Mediated AURKB Cleavage Promotes Cell Segregation and Tumorigenesis. Cell Rep. *26*, 3657–3671.e5.

41. Ding, L., Zhu, Q., Zhou, F., Tan, H., Xu, W., Pan, C., Zhu, C., Wang, Y., Zhang, H., Fu, W., et al. (2019). Identification of viral SIM-SUMO2-interaction inhibitors for treating primary effusion lymphoma. PLoS Pathog. *15*, e1008174.

STAR★METHODS

KEY RESOURCES TABLE

REAGENT or RESOURCE	SOURCE	IDENTIFIER
Antibodies		
Mouse monoclonal anti-PARP1	Santa Cruz	sc-8007
Mouse monoclonal anti-ZTA(ZEBRA)	Santa Cruz	sc-53904, clone BZ1
Mouse monoclonal anti-EBNA1	Santa Cruz	sc-57719, Clone 0211
Mouse monoclonal anti-LMP1	Kerafast	Cat.#: ETU001, S12
Mouse monoclonal anti-GAPDH	Proteintech	Cat.#: F1804
FITC anti-human CD3	Biolegend	Cat.# 300406
Brilliant Violet 510™ anti-human CD20	Biolegend	Cat.# 302340
antibodies of Fc inhibitor	Biolegend	Cat.# 422301
IRDye® 800cw Goat Anti-Mouse IgG	Li-COR	Cat.#: 926-32210
IRDye® 800cw Goat Anti-Rabbit IgG	Li-COR	Cat.#: 926-32211
Chemicals, peptides, and recombinant proteins		
PMSF	Amresco	Cat.#: 329-98-6
Aprotinin	Amresco	Cat.#: 9087-70-1
Leupeptin	Amresco	Cat.#: 103476-89-7
Pepstatin	Amresco	Cat.#: 26305-03-3
XenoLight D-Luciferin-K+	PerkinElmer	Cat.#: 122799
Cell Cycle and Apoptosis Analysis Kit	BioReagent	C1052
Z-DEVD-FMK	TargetMol	Cat.#: 210344-95-9
Cycloheximide	MCE	HY-12320
Annexin V-FITC/PI Apoptosis Detection Kit	YEASEN	40302ES60
Experimental models: Cell lines		
BJAB	Robertson ES Lab	Cai et al.[35]
E-BJAB	Lab stored	This paper
BL41	Robertson ES Lab	Saha et al.[36]
BL41-B95.8	Robertson ES Lab	Saha et al.[36]
DG75	Robertson ES Lab	Saha et al.[36]
DG75-EBV	Lab stored	This paper
Akata	Lu Jianhong Lab	NA
Akata-EBV	Lu Jianhong Lab	NA
LCL	Lab stored	Mo et al.[37]
BCBL1	Robertson ES Lab	Cai et al.[35]
KSHV-BJAB	Robertson ES Lab	Cai et al.[35]
C666-1	Lu Jianhong Lab	NA
5-8F	Lu Jianhong Lab	NA
JSC1	Robertson ES Lab	Cai et al.[35]
BC1	Robertson ES Lab	Cai et al.[35]
Software and algorithms		
Image Studio Lite Ver 5.2	LI-COR imaging systems	https://www.licor.com/bio/support/answer-portal/software/image-studio.html#SnippetTab

(*Continued on next page*)

Continued

REAGENT or RESOURCE	SOURCE	IDENTIFIER
SoftWorx Explore software	Applied Precision, Inc.	https://www.gelifesciences.com/en/us/shop/cell-imaging-and-analysis/highand-super-resolution-microscopes
Graphpad Prism 8	GraphPad Software	https://www.graphpad.com/
ImageJ Software	ImageJ Software	https://imagej.net/mbf/installing_imagej.htm

RESOURCE AVAILABILITY

Lead contact

Further information and requests for resources and reagents should be directed to and will be fulfilled by the Lead Contact, Qiliang Cai (qiliang@fudan.edu.cn).

Materials availability

This study did not generate any unique reagents.

Data and code availability

- Raw data has been deposited at Mendeley Data (https://data.mendeley.com/preview/mzbgk6gcd4).
- This paper does not report original code.
- Any additional information required to reanalyze the data reported in this paper is available from the lead contact upon request.

EXPERIMENTAL MODEL AND STUDY PARTICIPANT DETAILS

Human participants

Peripheral blood samples of five patients with hemophagocytic syndrome (9/3/2019 to 27/12/2019), and eight patients with diffuse large B-cell lymphoma (4 cases of EBV-positive lymphoma and four cases of EBV-negative lymphoma (9/12/2019 to 27/1/2021), were collected at Shanghai First People's Hospital (Table S1). Usage of redundant patient sample for research purpose was approved by the Medical Ethics Committee of the Institutional Review Board of Shanghai First People's Hospital (approval ID:2020SQ149). All patient samples of each donor gave written and signed the informed consent.

Cell lines

EBV-positive B-lymphoma LCL and EBV-negative B-lymphoma BJAB, DG75, Akata, and BL41 cell lines were purchased from ATCC and stored in the lab. DG75-EBV, Akata-EBV and BJAB-EBV were individually constructed by our laboratory (confirmed by fluorescence microscopy and Western blot experiments). DG75-EBV, Akata-EBV and BJAB-EBV cells were cultured with G418 (final concentration 250 μg/mL). BL41-B95.8, KSHV-positive B lymphoma cell lines K-BJAB and BCBL1, and EBV/KSHV double positive B lymphoma cell lines JSC1 and BC1 were kindly provided from Dr. Erle Robertson at University of Pennsylvania. EBV-positive nasopharyngeal carcinoma C666-1 and EBV-negative nasopharyngeal carcinoma 5-8F cell lines were kindly provided from Dr. Jianhong Lu at Southern Central University. The cell lines were all grown in RPMI 1640 medium containing 10% inactivated fetal bovine serum, penicillin and streptomycin at a final concentration of 100 μM, and 25 μg/mL gentamicin. All cell lines were incubated at 37°C in humidified environmental incubator with 5% CO_2.

Animals

Ethics statement and husbandry

All animal studies were conducted in accordance with the China Guide for the Care and Use of Laboratory Animals. All experiments were approved and supervised by the Institutional Animal Care and Use committee at Fudan University (approval ID: 20230707-003). Five-week-old female NOD/SCID mice were purchased from Beijing Vital River Laboratory Animal Technology Co., Ltd (Beijing, China). Mice were housed in microisolator cages with no more than five mice per cage at certified specific-pathogen-free or germ-free vivaria. Animals were provided with autoclaved water and food *ad libitum*.

METHOD DETAILS

High-throughput screening

The cells with viability higher than 95% were seeded in 384-well plates at 500 of cells/well in 50 μl fluid for 3 h and then treated with small molecules at 100 nM final concentrations in 0.1% DMSO for 72 h by a robot operator (autoTM liquid handling system) adding compounds (1,988 FDA-approved small-molecule drugs and 2,000 natural products provided by drug screening core facility at department of Chemistry, Fudan University of School of Basic Science Medicine) from 384-well drug plate, each experiment was duplicated. The initial concentration of

each drug compound was 100 μM, and 50 ng of each compound was dipped in the sample needle and added to 50 μl of the cell fluid, the final concentration of the compound was 100 nM. Cells treated with 0.1% DMSO and PBS were used as negative controls. After incubation, the 384-well plate were taken out and added 20 μl CellTiter-GloR for 30 min at room temperature to each well in the dark for automatically counting live cells with fluorescence staining (Quattro Micro reader, Waters), and results were analyzed with the MetaboScape analysis software. The number of live cells in the DMSO control was set as 100% and used to normalize cells treated with different compounds. A total of 94 hits that presented at least 50% cytotoxicity to LCL/E-BJAB cells but less than 10% cytotoxicity to BJAB cells were selected from the first round of screening, and then validated in a secondary screening, resulting in the selection of 31 final compounds.

Cell proliferation assay

An initial density of 100,000 cells per 5 mL RPMI 1640 medium for each cell line was seeded into a T25 culture flask and treated with different reagents, including DMSO, CetB, Thio, Cela, were counted daily using Vi-cell XR (Beckman Coulter).

Cytotoxicity assay *in vitro*

A total of 5,000 cells were seeded into a 96-well plates with 100 μl RPMI 1640 medium, and treated with different concentration of reagents, including DMSO, CetB, Thio, and Cela. After incubation for 48 h, 10 μl CCK-8 solution was added to each well. After 1 h, absorbance at a wavelength of 450 nm was read using Flexstation apparatus (MD).

Quantitation of EBV episome DNA

Total DNA was extracted by lysing buffer (10 mM Tris-HCl pH 8.0, 150 mM NaCl, 10 mM EDTA, 1% SDS) followed by proteinase K digestion. The copy number of EBV episomal DNA was detected by quantitative PCR targeting EBNA1 amplicon 387 bp with primers: F: 5′-CCTGTAGGGGAAGCCGAT-3′, R: 5′-CAATGGTGTAAGACGACATT-3′. The pET-28a plasmid carry EBNA1 DNA was used as a standard control. Relative gene expression levels were calculated by using the threshold cycle ($2^{-\Delta\Delta CT}$) formula.

Establishment of clinical EBV-infected B-lymphoma cell lines

EBV viral particles were isolated from the plasma of patients with hemophagocytic syndrome by ultracentrifugation, and used to infect BJAB cells at a MOI (multiplicity of infection) of 5 in a tissue culture incubator. The efficiency of BJAB cells with wild-type EBV infection was verified and confirmed by western blotting assay.

Cell cycle and apoptosis assay

The cell cycle was analyzed as previously described (Mo et al.[38]). Briefly, cells were harvested, washed twice with PBS, and resuspended at $1x10^6$ cells per ml. The fixed cells with cold 70% ethanol were then washed twice with PBS and resuspended in propidium iodide (PI) staining solution (50 μg/mL) and RNase A (100 ng/mL) for 30 min at room temperature. $1x10^4$ PI-stained cells were subjected to flow cytometry using a BD FACS Calibur. The data were analyzed using FlowJo software. For cell apoptosis assay. Annexin V-FITC/PI Apoptosis Detection kit (Cat.# 40302ES60) was used in this experiment. Briefly, $1x10^6$ cells were harvested, washed twice with PBS, and resuspended with 100 μL Binding Buffer. Then, cells were resuspended in 5 μL Annexin V-FITC and 10 μL PI Staining Solution for 10-15 min in dark light. $1x10^6$ Annexin V-FITC/PI-stained cells were subjected to flow cytometry using a BD FACS Calibur.

Flow cytometry analysis of human PBMC

The flow cytometry antibodies of Fc inhibitor (Fc Receptor Blocking Solution, Cat.# 422301), CD3 (FITC anti-human CD3 antibody, Cat.# 300406) and CD20 (Brilliant Violet 510™ anti-human CD20 antibody, Cat.# 302340) used in this study were purchased from Biolegend, USA. A total of 1 $x10^6$ human peripheral blood mononuclear cells (PMBC) were harvested, washed twice with cell lotion (PBS with 2% BSA), and resuspended with 100 μL cell lotion. 5 μL Fc inhibitor was added and incubated for 5-10 min, then 5 μL CD3 and 5 μLCD20 were added and incubated in ice for 15 min away from light. Before human PBMC were subjected to flow cytometry using a BD FACS Calibur, they were washed twice with cell lotion. The data were analyzed using FlowJo software.

Immunoblotting assay

Immunoblotting analyses were performed as described previously (Han et al.[39]). Briefly, cells were harvested and lysed in the radioimmunoprecipitation assay (RIPA) buffer containing protease inhibitors (Sigma-Aldrich). Proteins were separated by SDS-polyacrylamide gel electrophoresis gels and transferred to 0.45-mm nitrocellulose membrane (Millipore). The membrane was probed with the primary antibodies as indicated and appropriate IRDye-800CW conjugated secondary antibodies, and scanned with an Odyssey Infrared scanner (LiCor Biosciences).

Immunofluorescence

Immunofluorescence assays were performed as described previously (Zhu et al.[40]). Briefly, cells were harvested and plated in polylysine-treated coverslips for 4 h in CO_2 incubator to let cells attach to the plate followed by washing with ice-cold PBS twice, and fixed in 4%

paraformaldehyde for 20 min at room temperature. After fixation, cells were washed three times in PBS and permeabilized in PBS containing 0.2% fish skin gelatin (G-7765; Sigma) and 0.2% Triton X-100 for 5 min, followed by primary (anti-EBNA1) and secondary antibody staining. Nucleus was counterstained with 4, 6-diamidino-2-phenylindole (DAPI), and coverslips were mounted with p-phenylenediamine. The images were analyzed with Photoshop (Adobe Systems Inc., San Jose, CA, USA) and fluorescence was quantified with the ImageJ software.

Soft agar colony formation

Soft agar colony formation assay was performed as described previously (Zhu et al.[40]). Briefly, the bottom layer containing 0.75% agar in 10% FBS RPMI1640 were prepared first, and then the top layer contains appropriate amounts of cells in 0.36% agar mixture were put on the bottom layer. The dish containing 2 layers was maintained in 37°C incubator for 2 weeks, and then the colonies were stained with 8 mg/ml NBT (Nitrotetrazolium Blue Chloride) in ddH_2O and were cultured at 37°C overnight. Colonies were quantified with the ImageJ software.

Quantitative PCR

Quantitative PCR (qPCR) assay was performed as described previously (Mo et al.[38]). Total RNA was extracted from cells using TRIzol (Invitrogen), processed for cDNA synthesis using the Reverse Transcription Kit (Applied Biosystems), and subjected to qPCR by using SYBR Green Master Mix (Applied Biosystems). According to manufacturer's protocol, PCR conditions were performed as steps below: 1 cycle at 95°C for 5 min, followed by 40 cycles of 95°C for 15 s, 60°C for 30 s and 72°C for 30 s. A melting-curve analysis was performed to verify the specificities of the amplified products. The values for the relative levels of change were calculated by the threshold cycle (ΔΔCT) method, and samples were tested in triplicates. The oligo sequences of primers targeting EBNA1 (F:5′-CCAAGAAGGTGGCCCAGATGGTGAG-3′; R:5′-TCACTCCTGCCCTTCCTCACCC TC-3′) and GAPDH (F:5′-CTGGGCTACACTGAGCACC-3′; R: 5′-AAGTGGTCG TTGAGGGCAATG-3′) were used, respectively.

Tumor xenograft

For the tumor formation experiment, 24 female NOD/SCID mice (Beijing Vital River Laboratory Animal Technology Co., China) at 5 weeks old were each intraperitoneally injected with $1.5x10^7$ LCL-Luc cells. At day 8 post-inoculation, mice were intraperitoneally injected with D-luciferin at 150 mg/kg body weight and imaged with an IVIS Spectrum *in vivo* imaging system (PerkinElmer). Equal of ROI (the region-of-interest) signals based on the (p/s)/(microwatts per square centimeter) formula were randomly split into 5 groups, and individually treated with PBS, DMSO, CetB (5 mg/kg), Cela (3 mg/kg), combined CetB (2.5 mg/kg) with Cela (1.5 mg/kg) every other day for 6 times, and all groups were weighted once every other day. At week 2 post-treatment, live imaging was performed again. For Matrigel tumor, 10 female BALB/c-nu mice (Beijing Vital River Laboratory Animal Technology Co., China) at 5 weeks old were each subcutaneously injected with $1.0 x10^7$ cells (which were suspended in mixture of 100 μl RPMI1640 with sera free and 100 μl Matrigel) on the right groin for BL41-B95.8 cells and the left groin for BL41 cells, respectively. At day 7 post-inoculation, equal of weight based on the formula were randomly split into 2 groups, and individually treated with PBS/DMSO or CetB (5 mg/kg) every other day for five times, and all groups were weighted once every other day. At week 2 post-treatment, all mice were euthanized and subcutaneous tumors were extracted for weight and size measure. All animal studies were conducted in accordance with China guide for the Care and Use of Laboratory Animals. All experiments were approved and overseen by the institutional animal care and use committee at Fudan University.

QUANTIFICATION AND STATISTICAL ANALYSIS

Data are expressed as mean ± standard deviation (SD). The significance of the variability between different groups was determined by a two-way analysis of variance using GraphPad Prism software (version 8.0). A p-value of < 0.05 was considered statistically significant and a p-value of > 0.05 was considered statistically non-significant (Ding et al.[41]).